IMF dependence of high-latitude thermospheric wind derived from CHAMP cross-track accelerometer data

Matthias Förster

Helmholtz Zentrum Potsdam, Deutsches GeoForschungsZentrum (GFZ), Germany, mfo @ gfz-potsdam.de

ISSI Team of Adrian Grocott:

A statistical investigation into coupled magnetospheric - ionospheric dynamics via multi-scale, multi-instrument, data assimilation

CHAMP Spacecraft with Accelerometer

Launch: July 2001
Near-circular polar orbit
Height : ~400 km (2003)

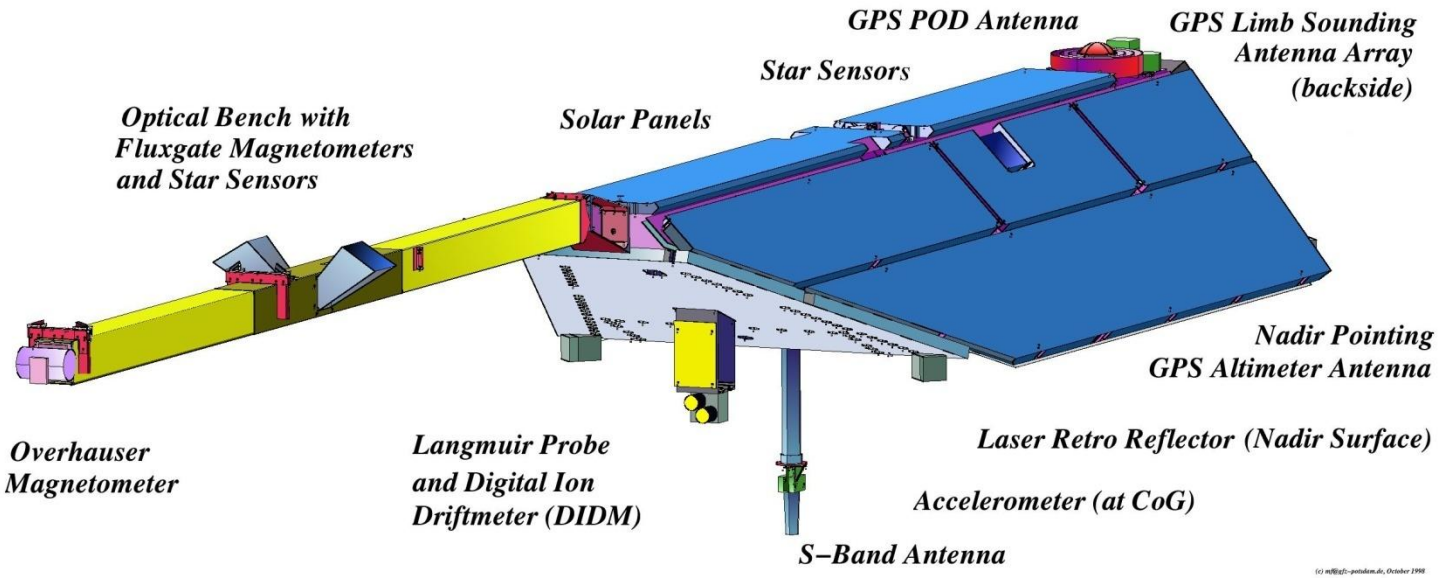

... enables highly precise measurements of non-gravitational accelerations to deduce the thermospheric density and cross-track wind velocity

$$\vec{a} = -\frac{1}{2}\rho\frac{C_d}{m}A_{eff}V^2\vec{v},$$

(drag acceleration)

$$\frac{V_y}{V_x} = -\frac{a_y}{a_x}. \quad \Rightarrow \quad U_{zonal} = V_y - V_c = -\frac{a_y}{a_x}V_x - V_c$$

(cross-track)

Reference:

Liu, H., Lühr, H., Watanabe, S., Köhler, W., Henize, V., and Visser, P. (2006): Zonal winds in the equatorial upper thermosphere: Decomposing the solar flux, geomagnetic activity, and seasonal dependencies, Journal of Geophysical Research, 111, A07307.

==> See also the ESA study report and the forthcoming paper of Eelco Doornbos et al. (2010)

CHAMP Mass Density Data

01 Jan – 31 Dec 2003, averaged

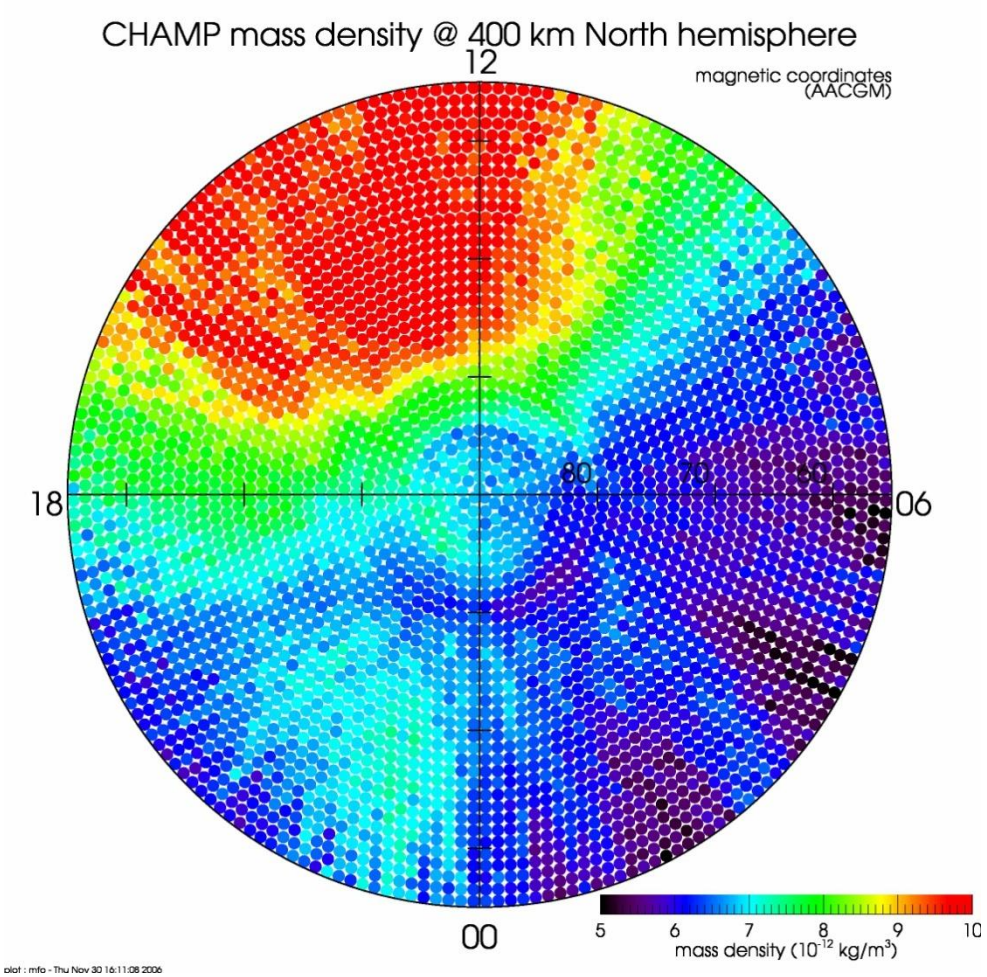

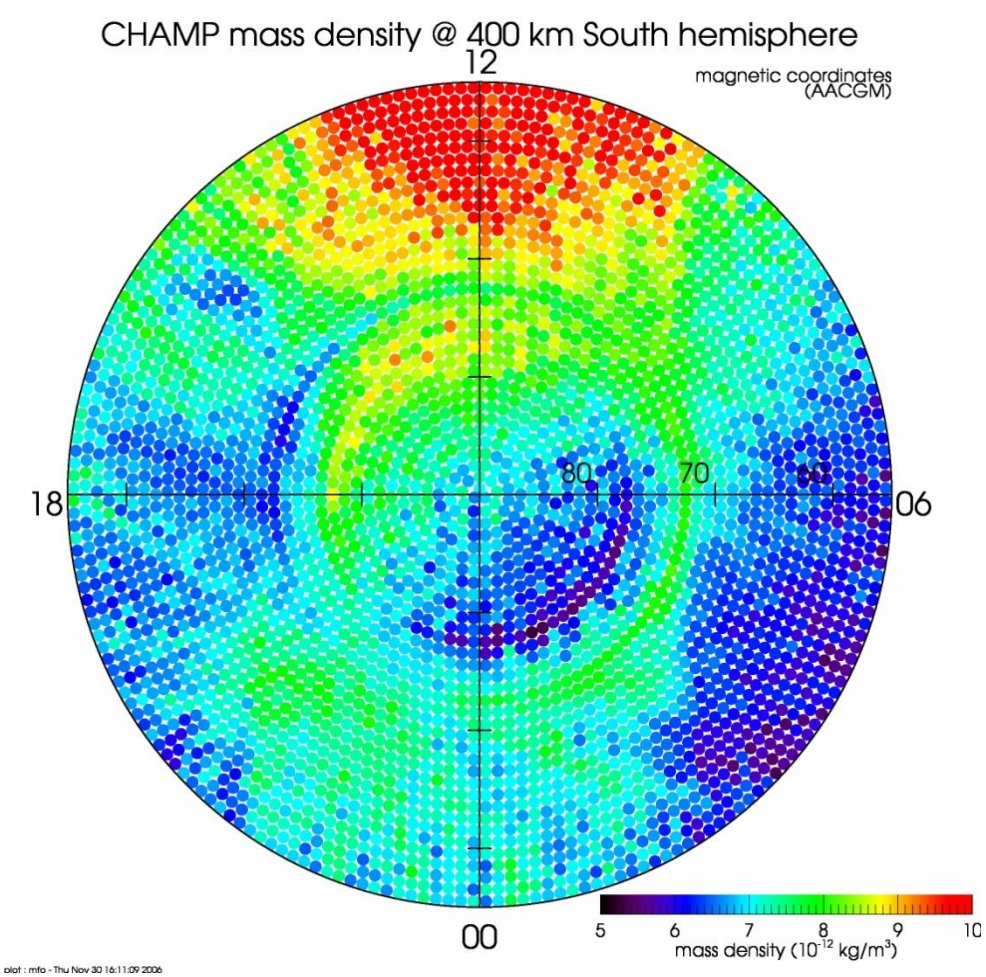

North Hemisphere **South Hemisphere**

(geomagnetic coordinates: AACGM)

Thermospheric Density & Wind

deduced from accelerometer data of CHAMP

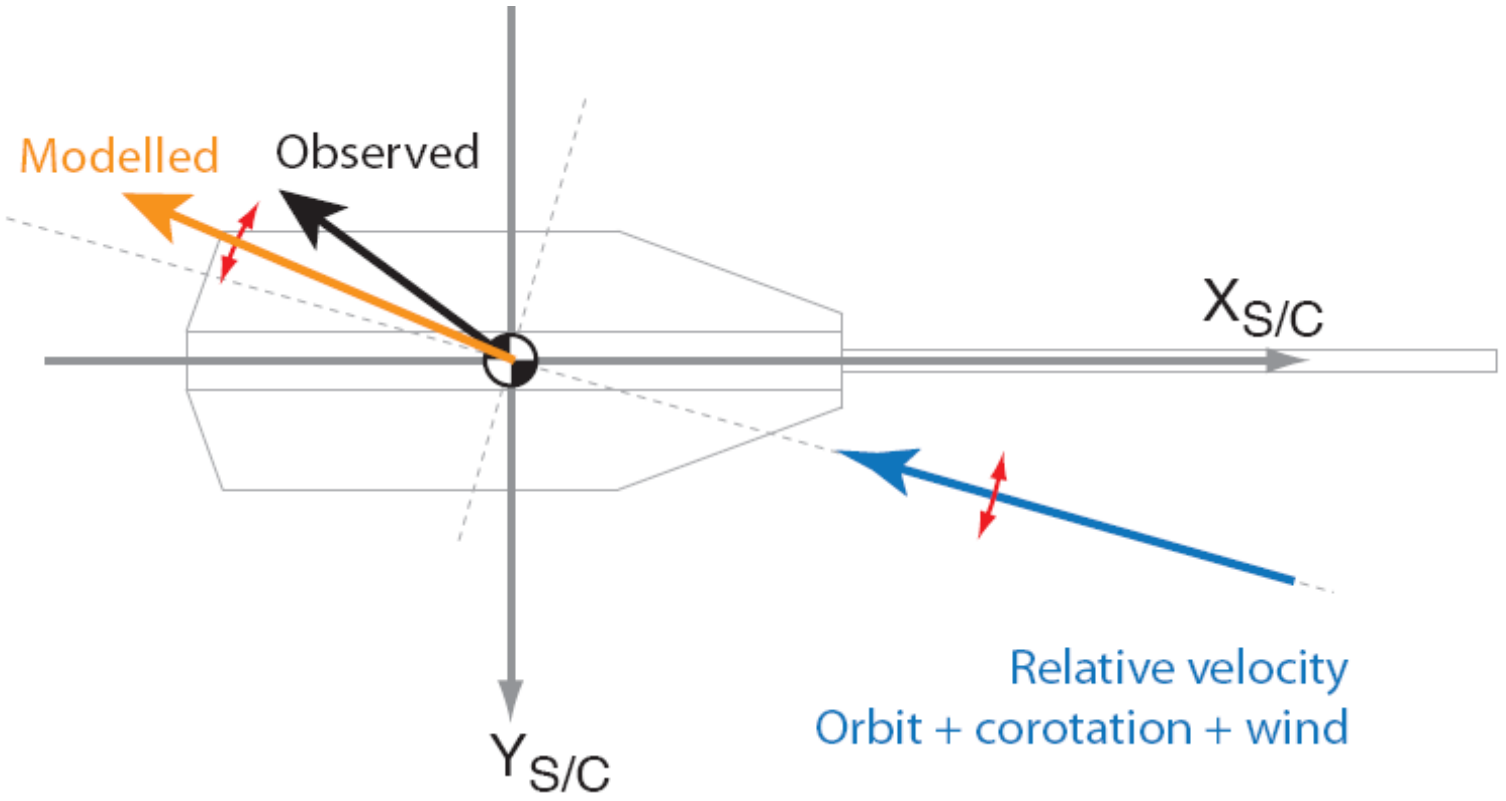

Iterative processing scheme to derive the thermospheric density and cross-track (one component) wind velocity from accelerometer measurements (CHAMP, GRACE, Swarm, …)

Outcome of a recent ESA study on: ‘Air density models derived from multi-satellite drag observations’ (21022/07/NL/HE)

CHAMP Spacecraft in the Air Stream

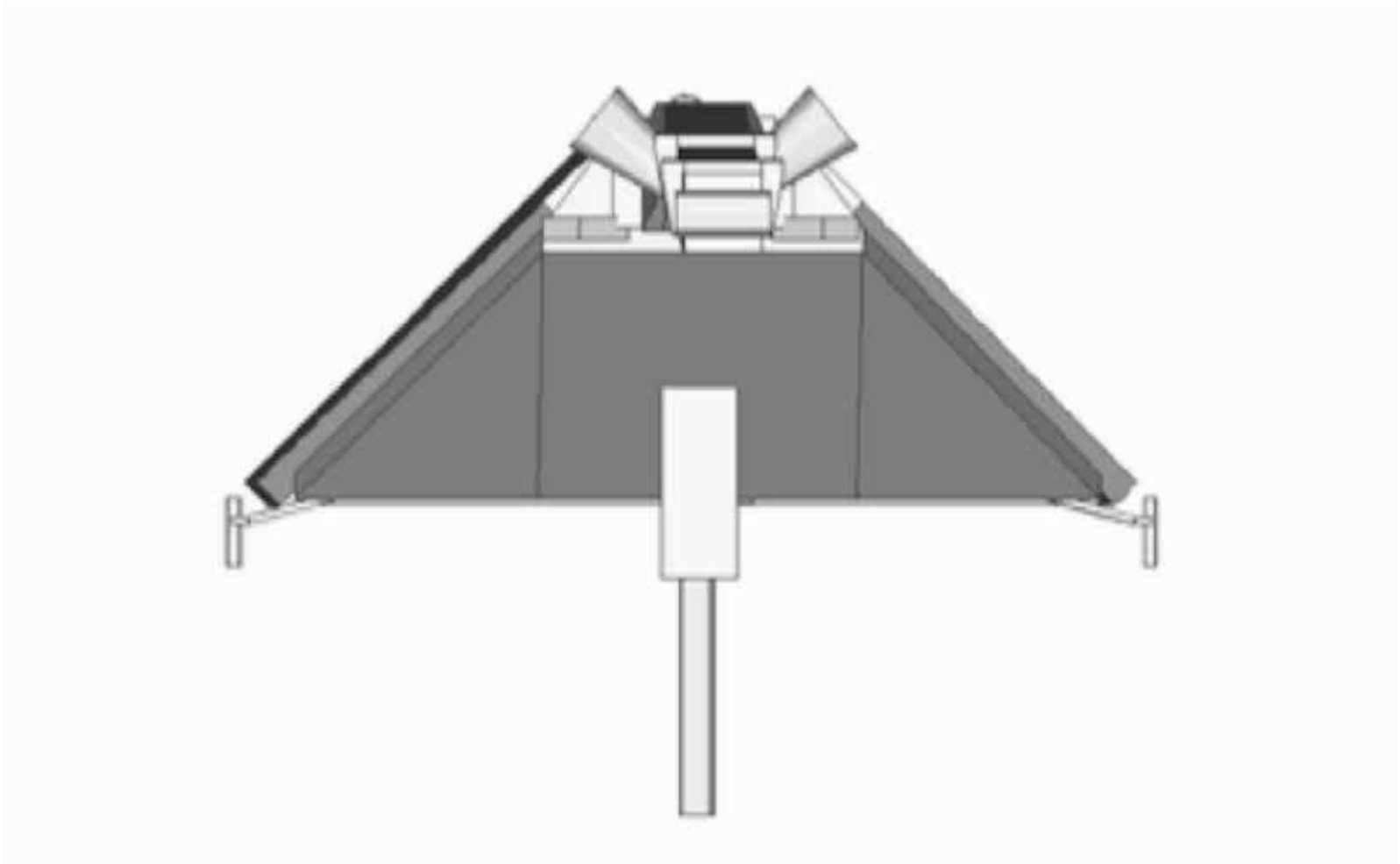

Corotation of the upper atmosphere (~490 m/s @ equator) plus
Thermospheric wind (from the HWM model) plus
Yaw, Roll and Pitch steering of the S/C

CHAMP Data Binning Schema

equal-area size bins, ~1 x 1 degrees

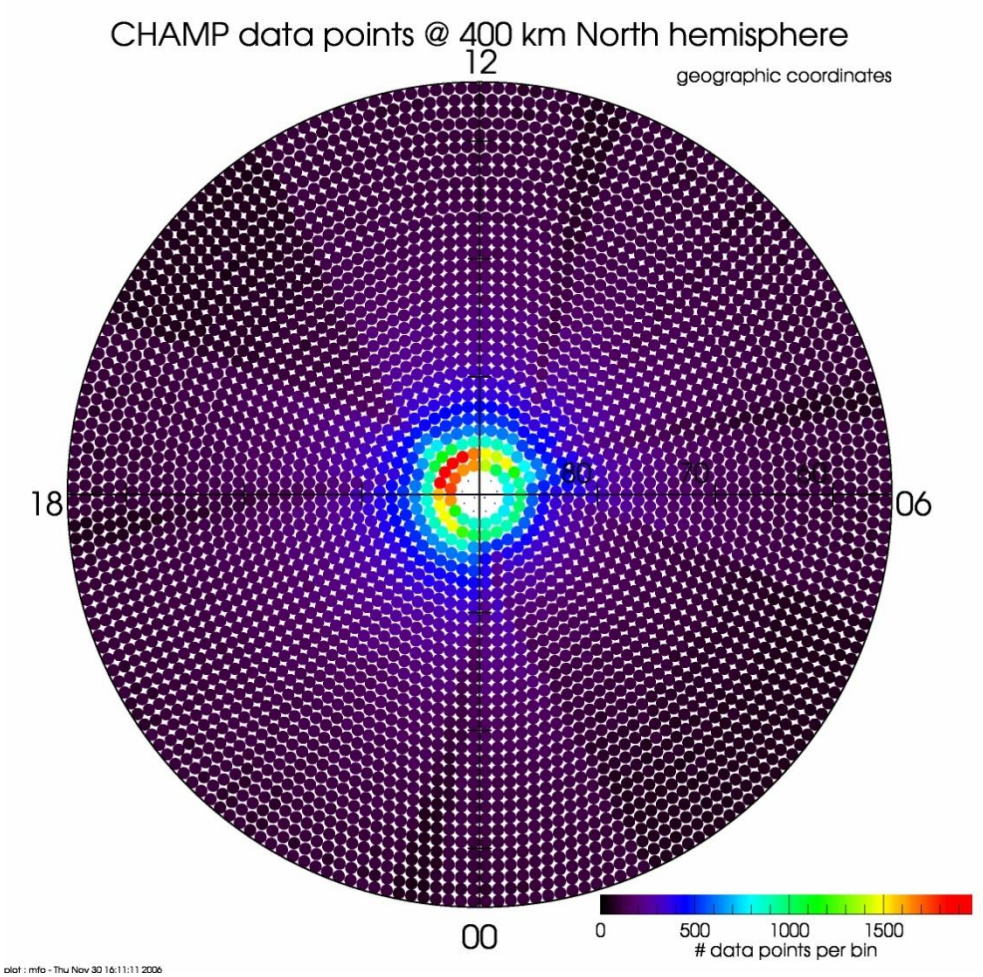

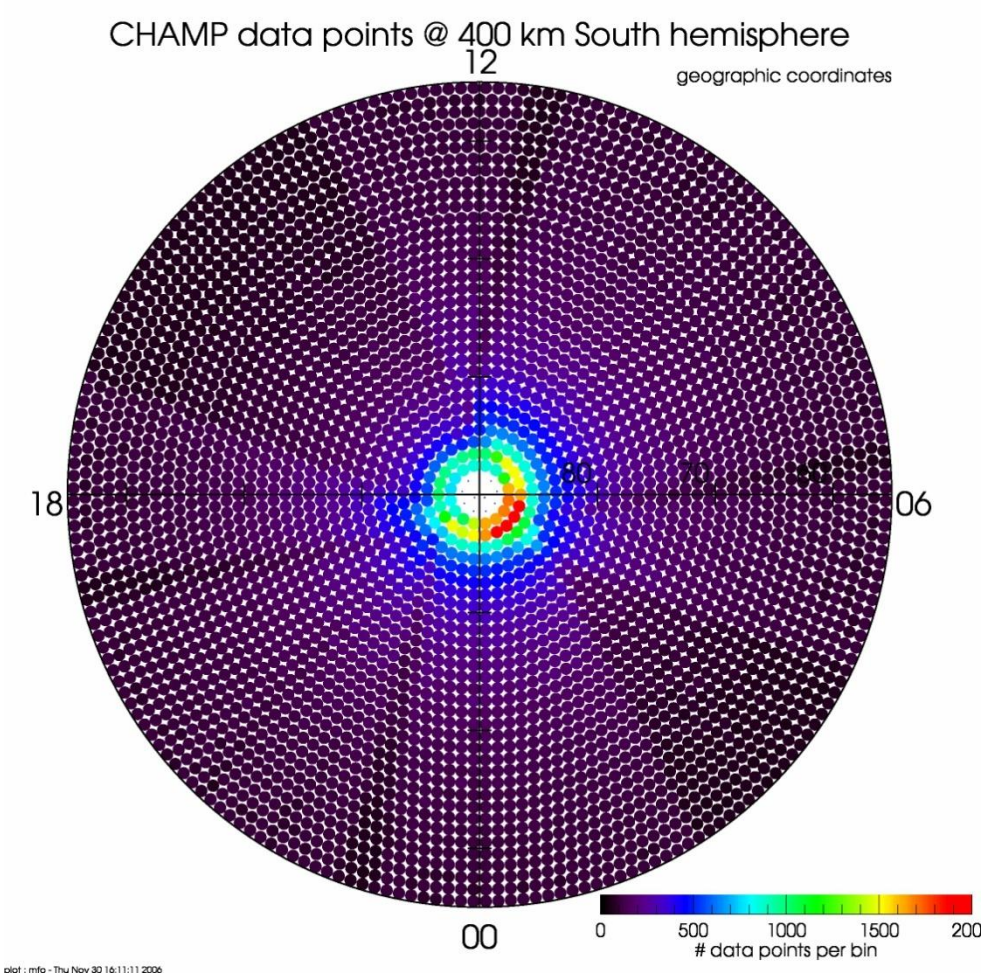

North Hemisphere **South Hemisphere**

(geographic coordinates)

CHAMP Data Binning Schema

equal-area size bins, ~1 x 1 degrees

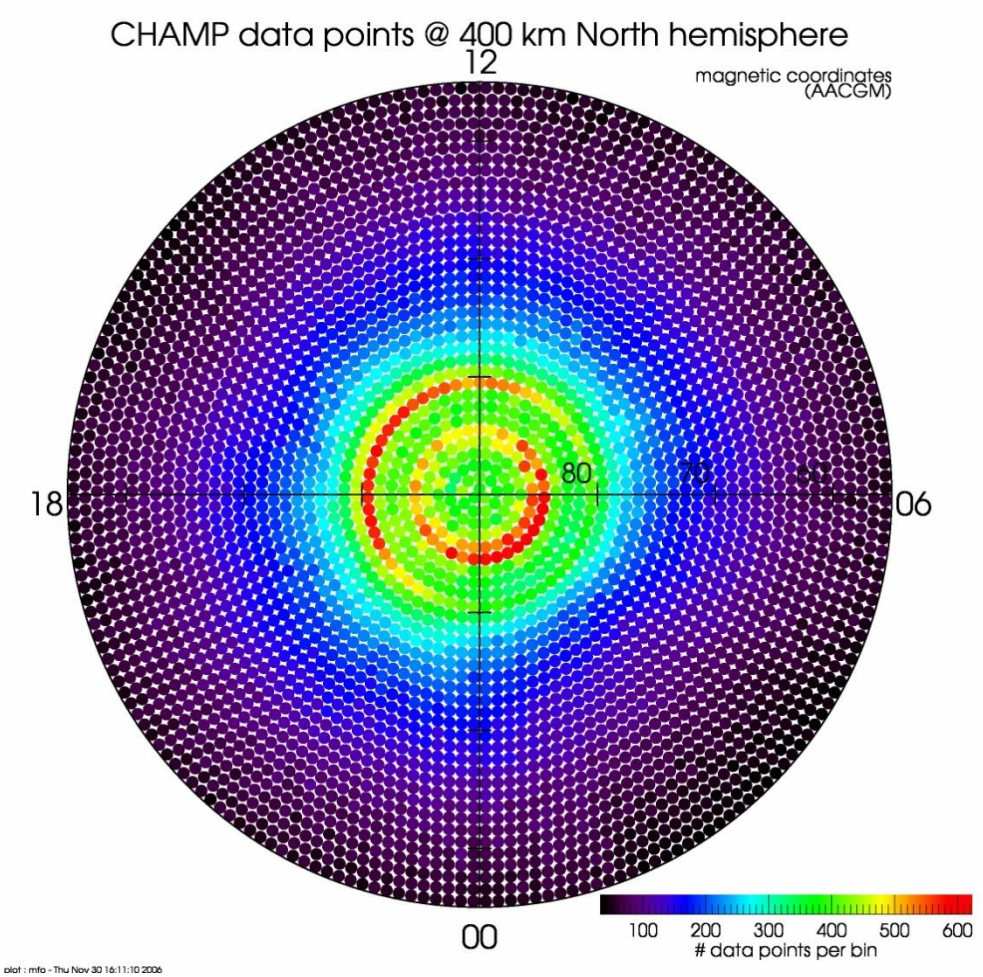

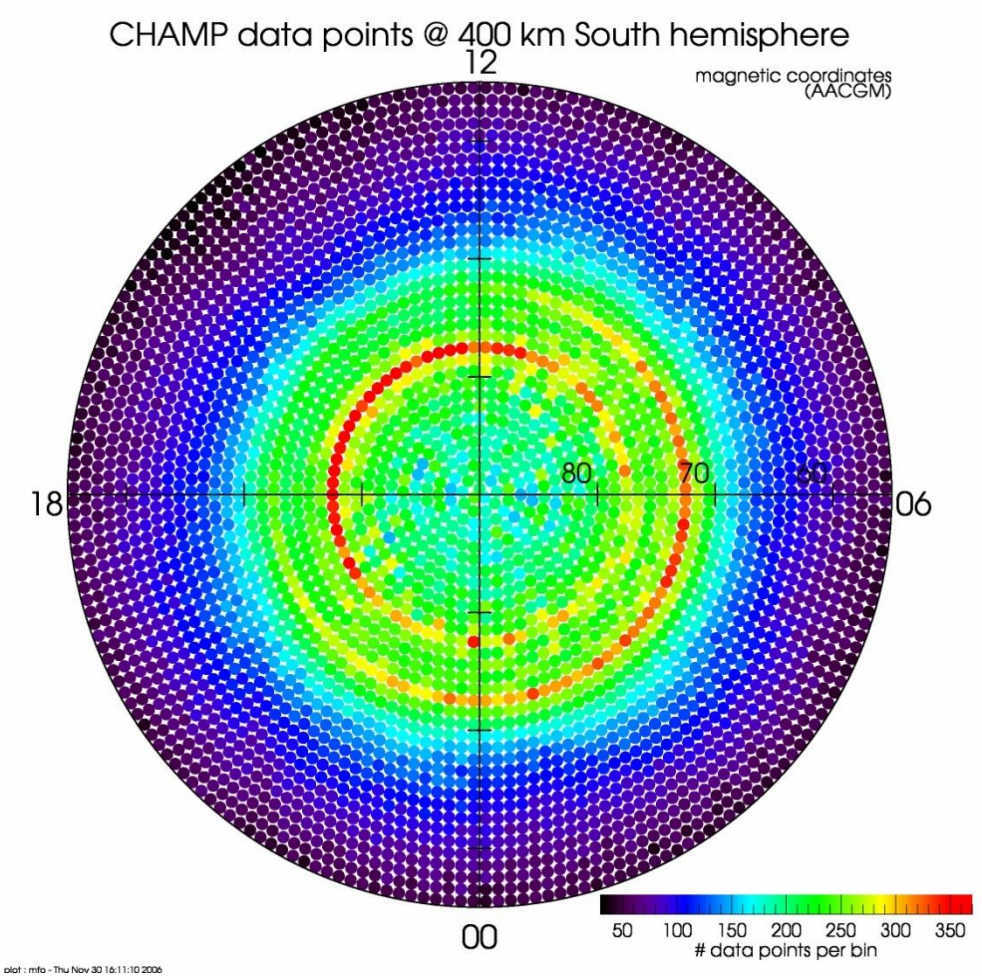

North Hemisphere **South Hemisphere**

(geomagnetic coordinates: AACGM)

Examples of Average Wind Vector Estimation

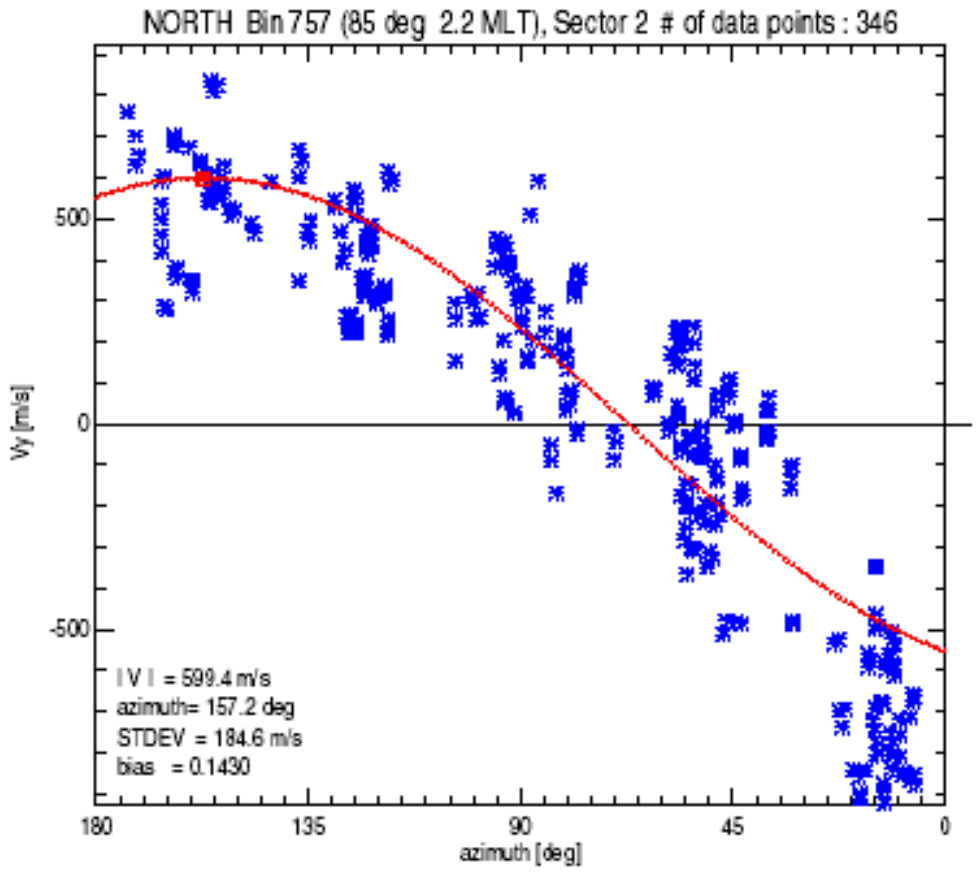

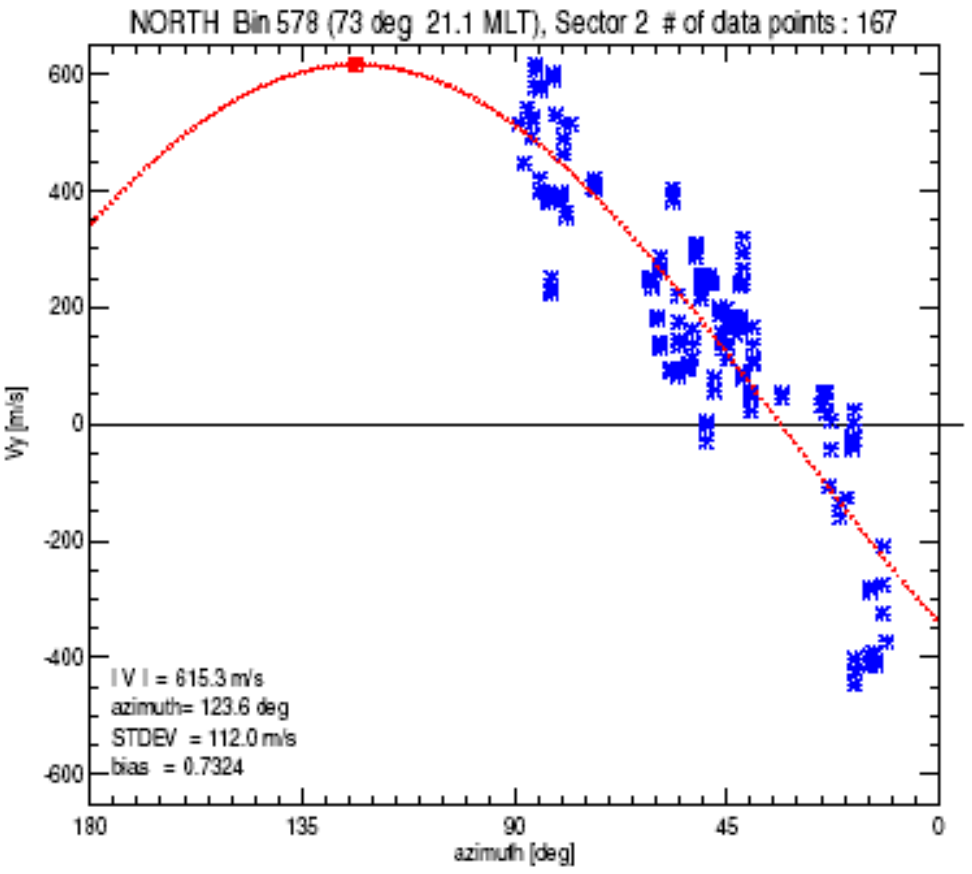

$$\sum_{i=1}^{n} \left(V_{yi} - \mathbf{k}_i \boldsymbol{V} \right)^2 = \delta f$$

V_{yi} - Observed cross-track wind component

$\mathbf{k}_i$ - and it unit vector direction

$\mathbf{V}$ - resultant wind vector

δf - minimization (Singular Value Decomposition)

Bias Value of Wind Vector Distribution

equal-area size bins, ~2 x 2 degrees

North Hemisphere

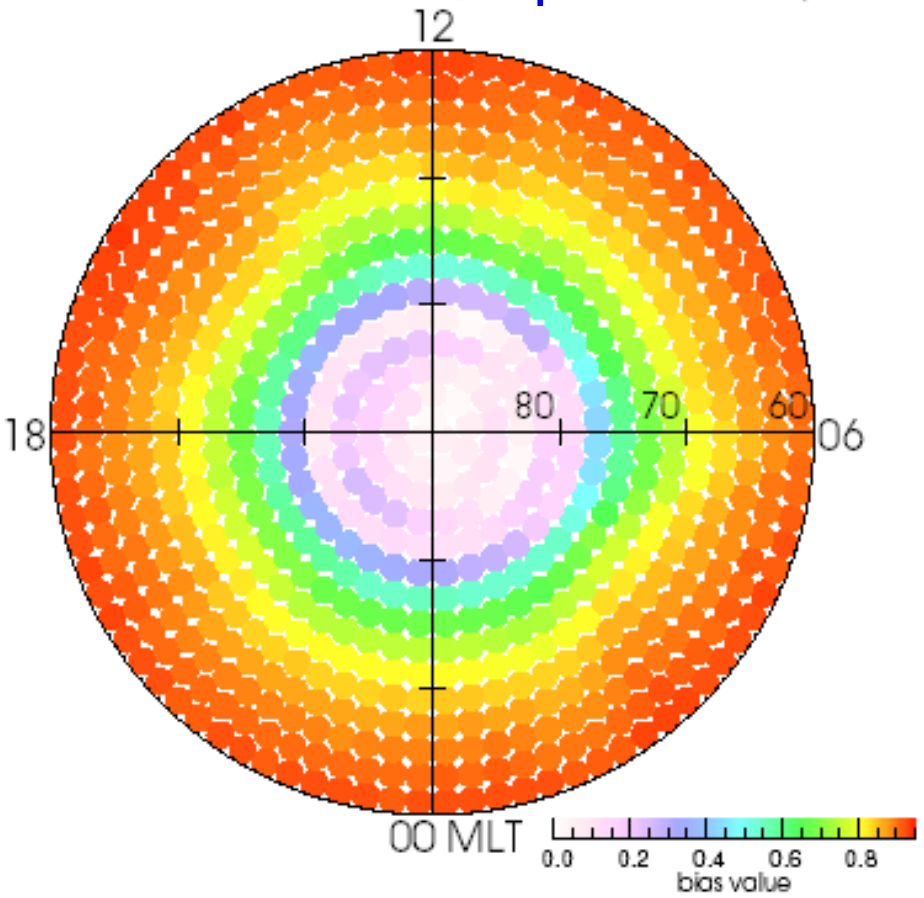

South Hemisphere

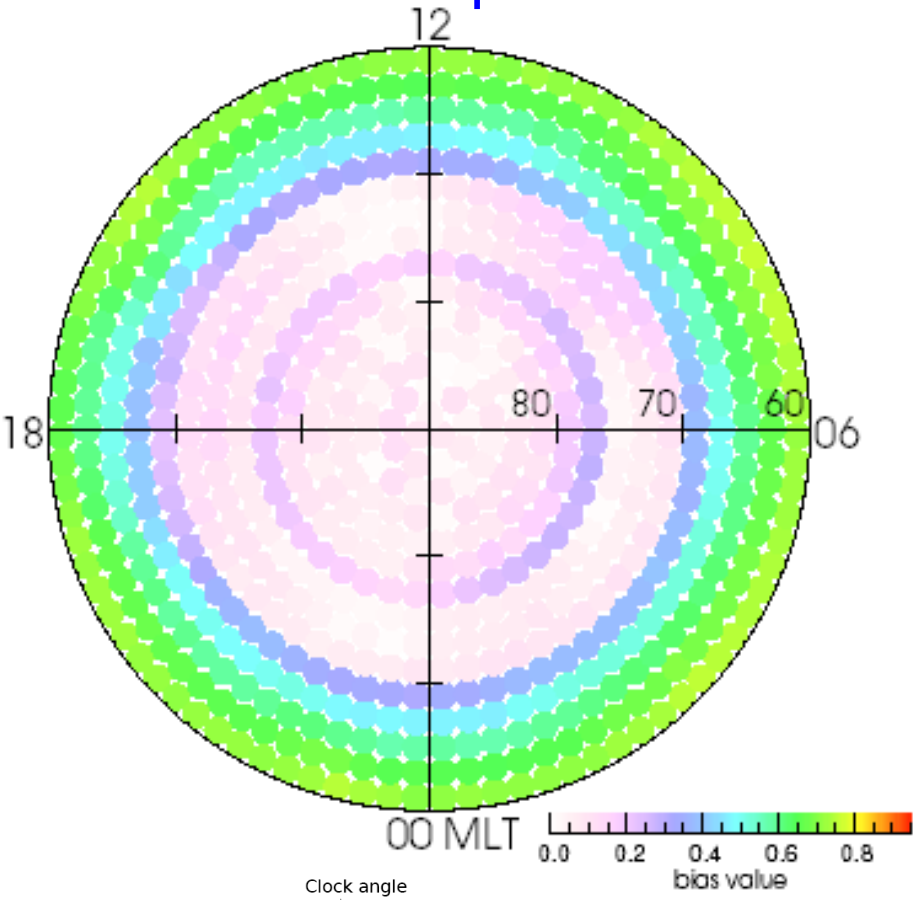

Principle of bias vector & value estimation :

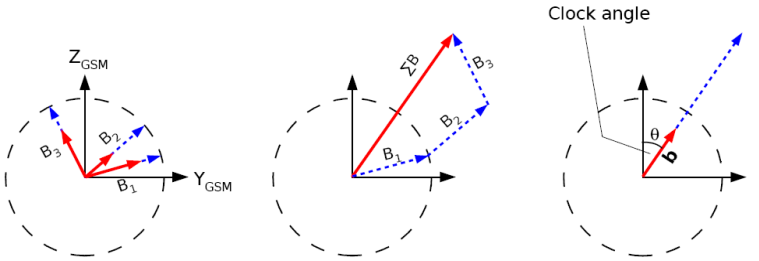

The High-latitude Wind Pattern

…driven by EUV, Joule and particle heating, and ion drag

Overall average of the cross-polar thermospheric wind circulation:

North Hemisphere

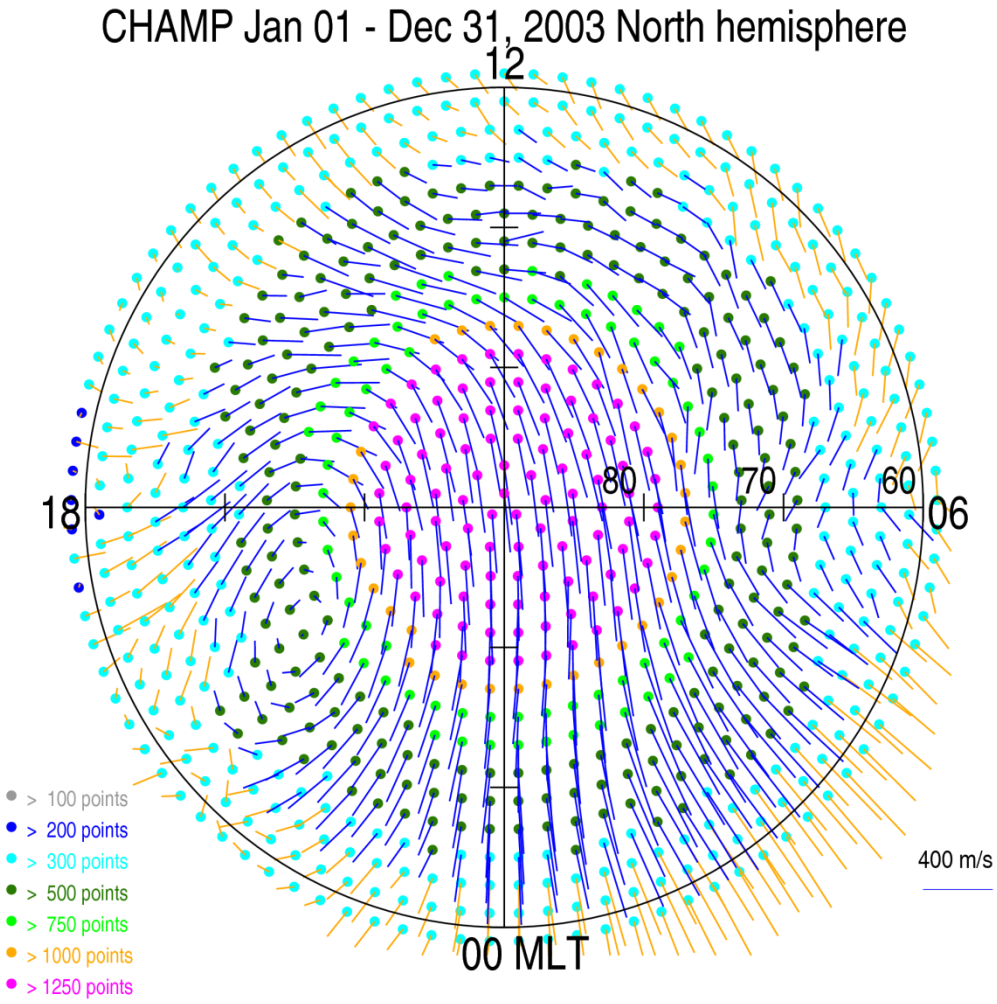

South Hemisphere

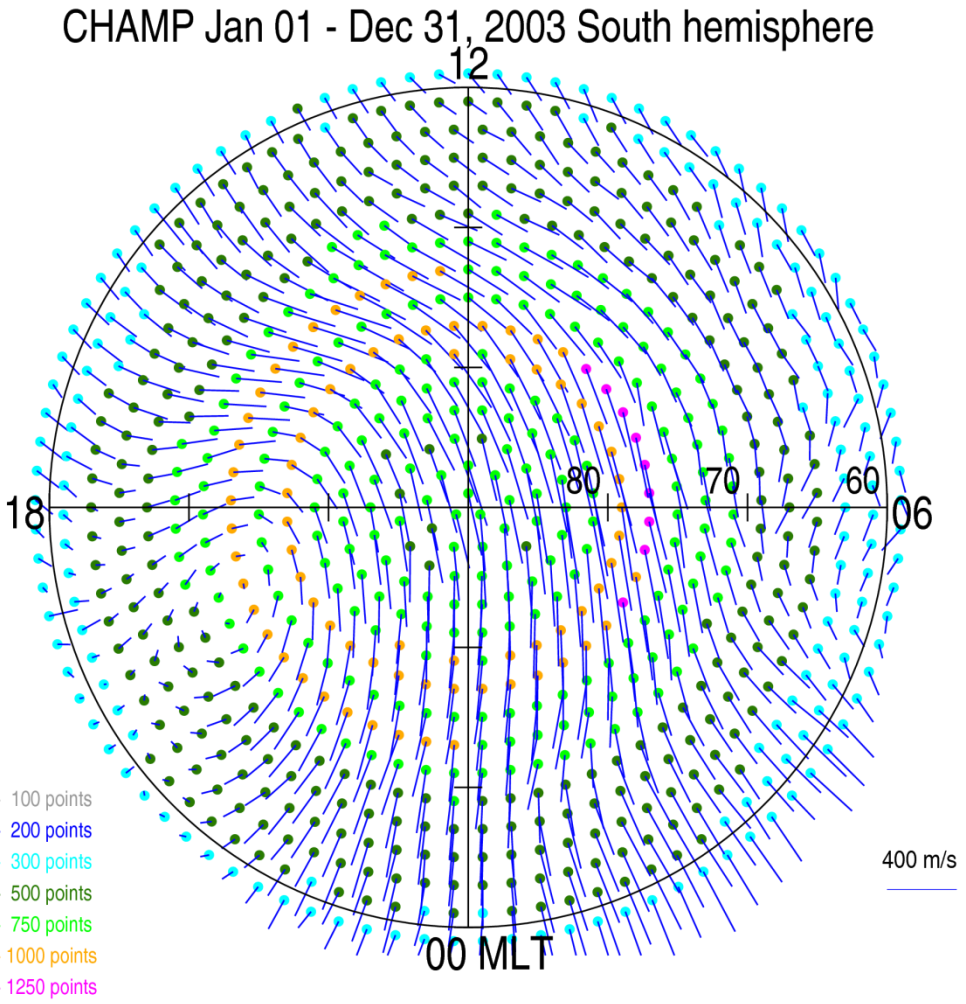

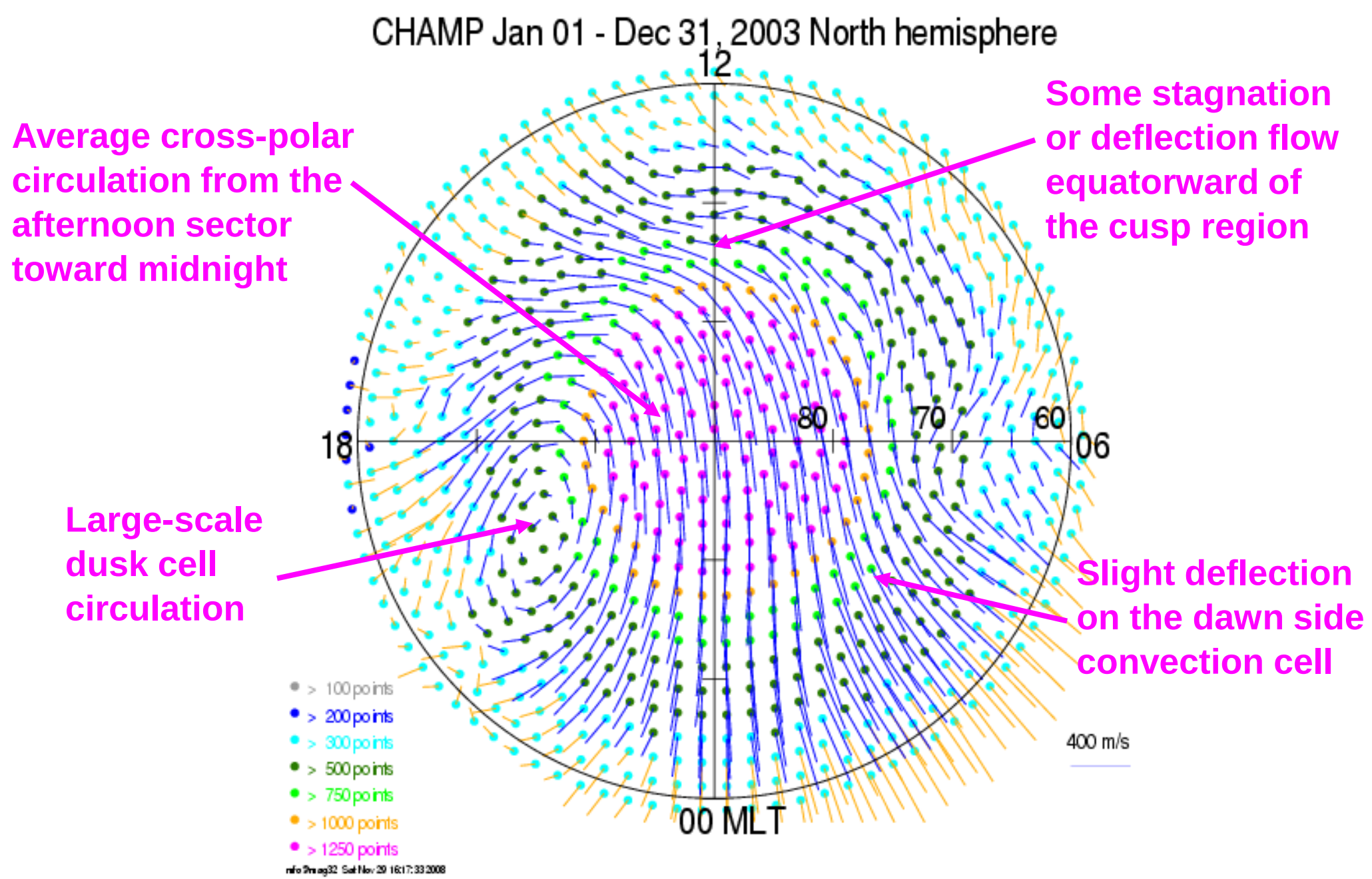
CHAMP Jan 01 - Dec 31, 2003 North hemisphere
12
18
06
00 MLT
80
70
60
Average cross-polar circulation from the afternoon sector toward midnight
Some stagnation or deflection flow equatorward of the cusp region
Large-scale dusk cell circulation
Slight deflection on the dawn side convection cell
400 m/s
> 100 points
> 200 points
> 300 points
> 500 points
> 750 points
> 1000 points
> 1250 points

Plasma Convection

Deduced from Cluster EDI measurements

Upstream IMF conditions :
SW propagation – Weimer method

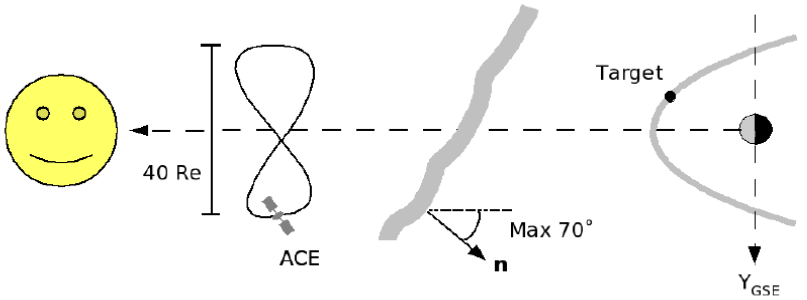

$$\Delta t = \frac{(\mathbf{r}_{ACE} - \mathbf{r}_{TARGET}) \cdot \mathbf{n}}{\mathbf{V}_{ACE} \cdot \mathbf{n}}$$

Weimer et al., J. Geophys. Res. Vol. 108, doi: 10.1029/2002JA009405, 2003; with Correction Dec 2004
Haaland, S., G. Paschmann, and B.U.Ö. Sonnerup, J. Geophys. Res., Vol. 111, doi: 10.1029/2005JA011376, 2006

- Determine upstream IMF conditions, measured by ACE at L1
- Remove intervals with ‘unstable’ IMF by bias vector filtering
- Map spatially distributed EDI measurements into ionosphere
- Transform binned pattern into usual potential plots

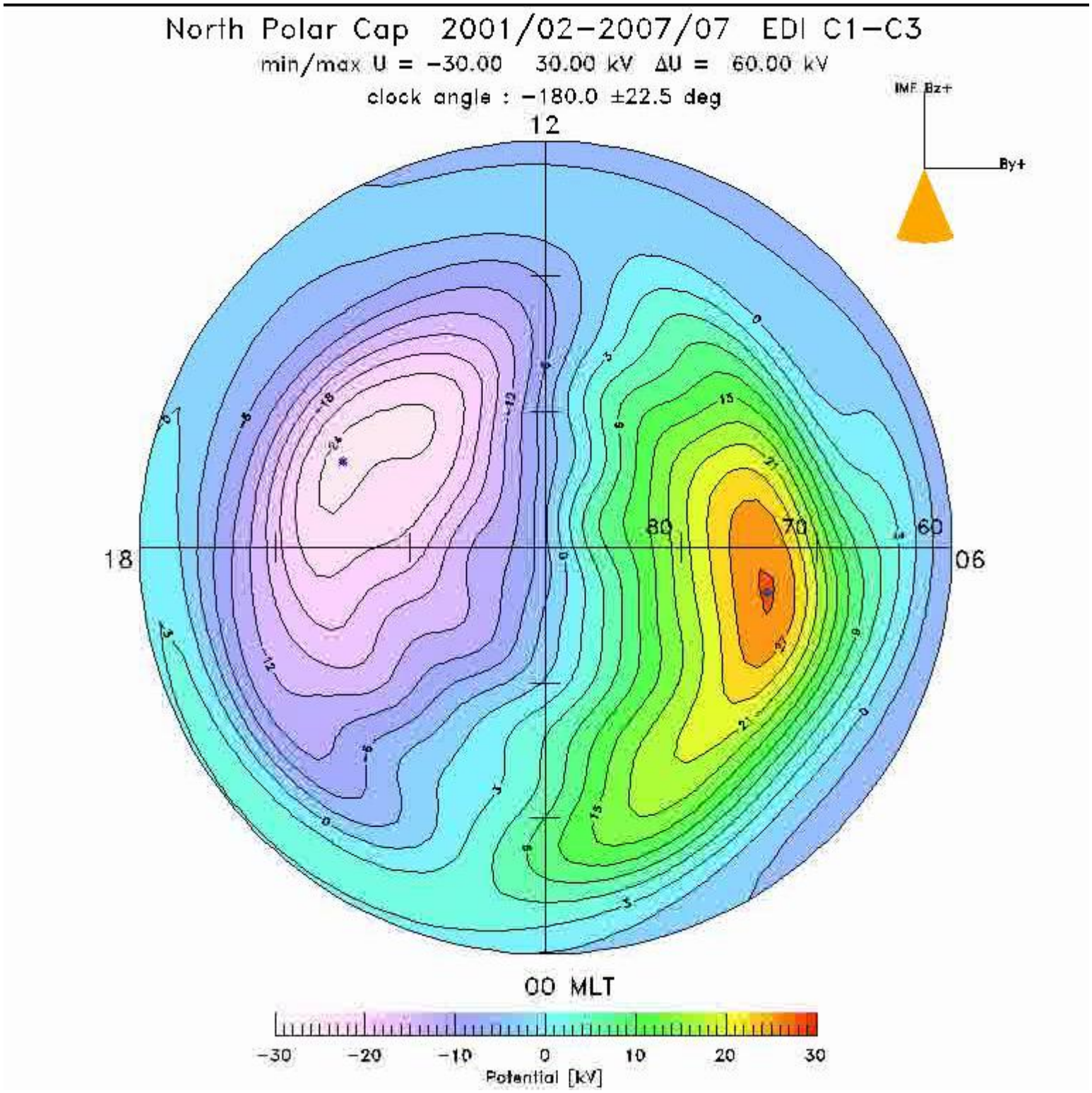
North Polar Cap 2001/02–2007/07 EDI C1–C3
min/max U = −30.00 30.00 kV ΔU = 60.00 kV
clock angle : −180.0 ±22.5 deg
IMF Bz+
By+
12
18
06
00 MLT
80
70
60
−30
−20
−10
0
10
20
30
Potential [kV]

North Hemisphere

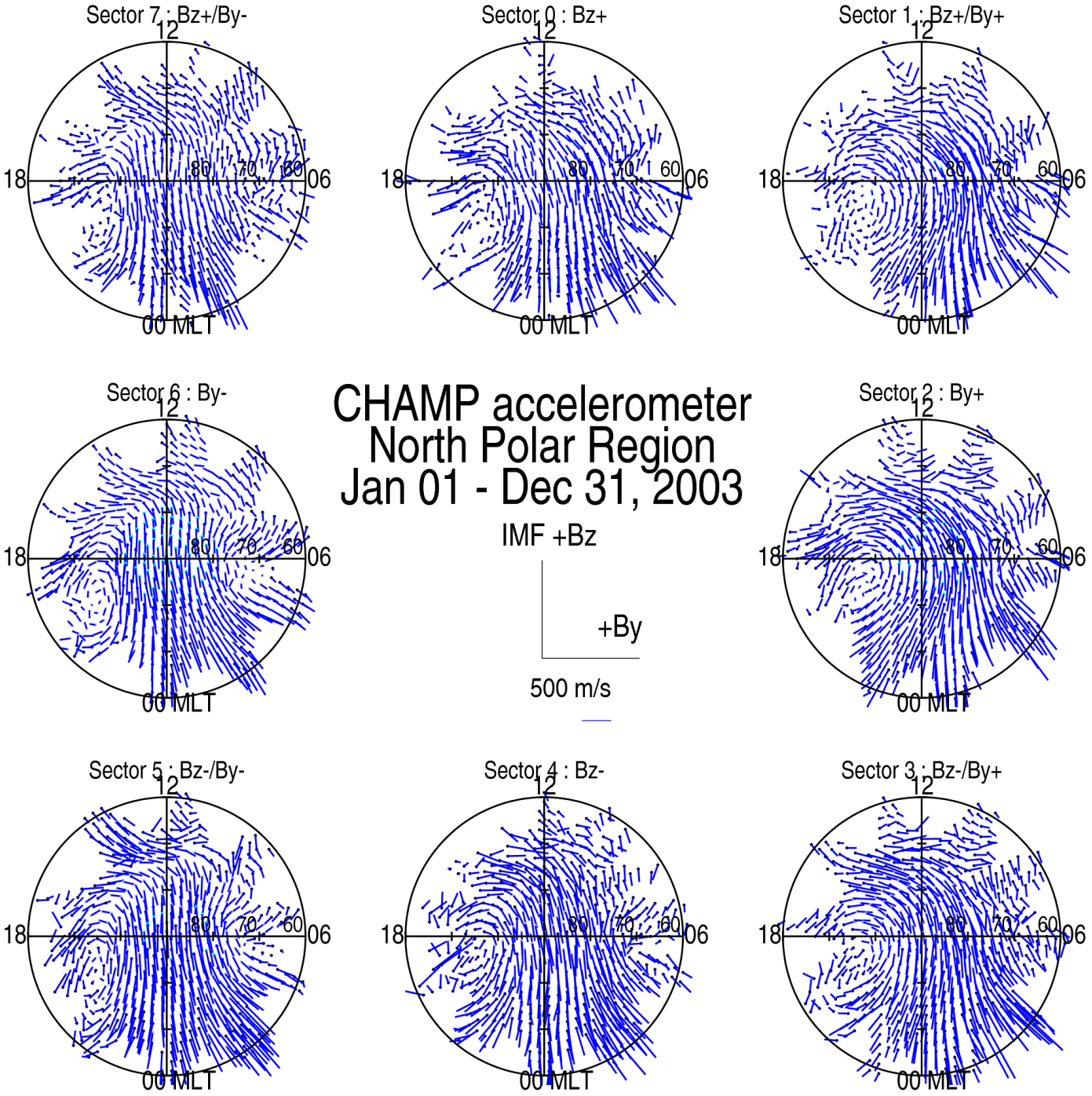

South Hemisphere

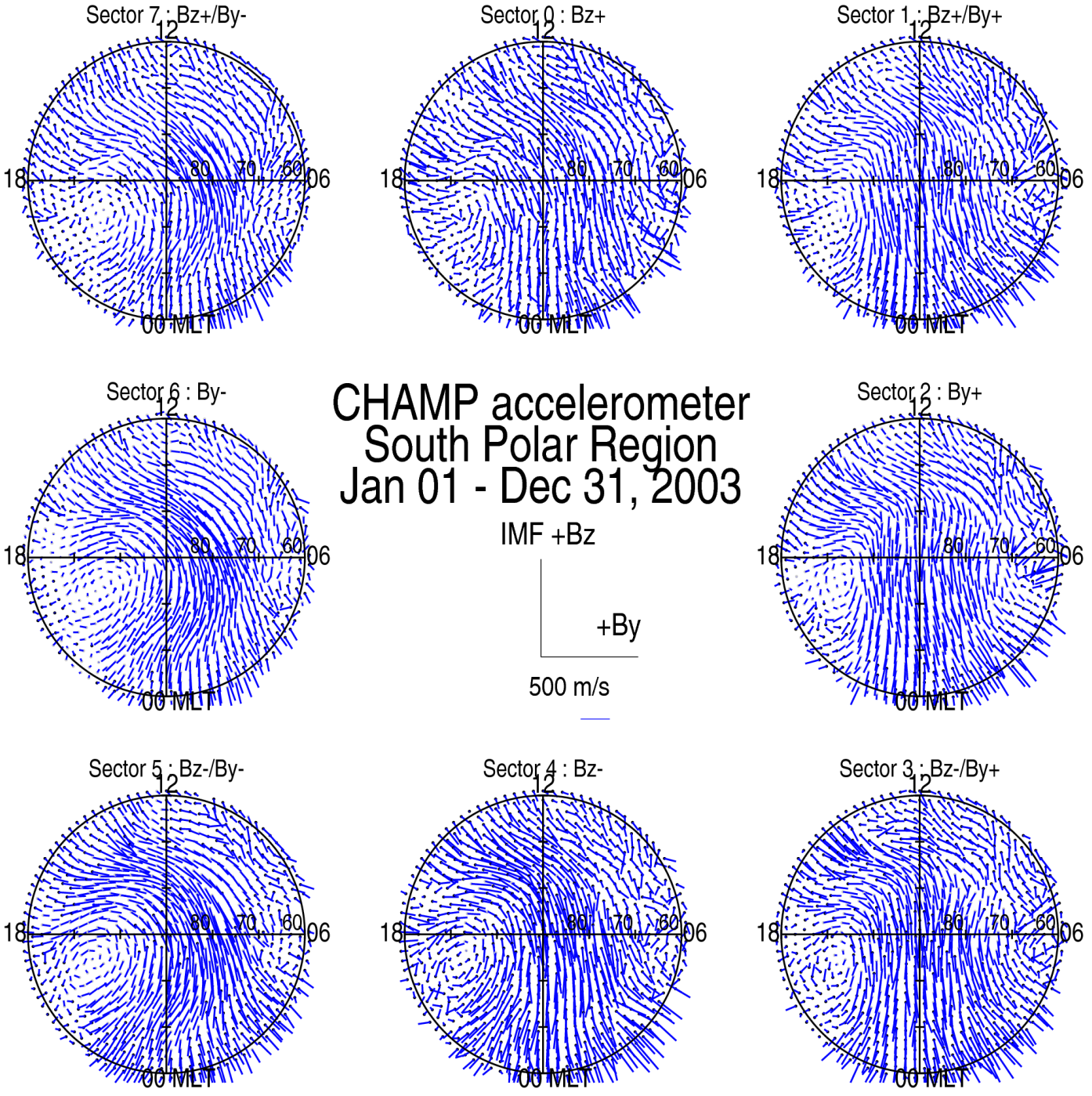

North Hemisphere

Neutral wind (CHAMP)

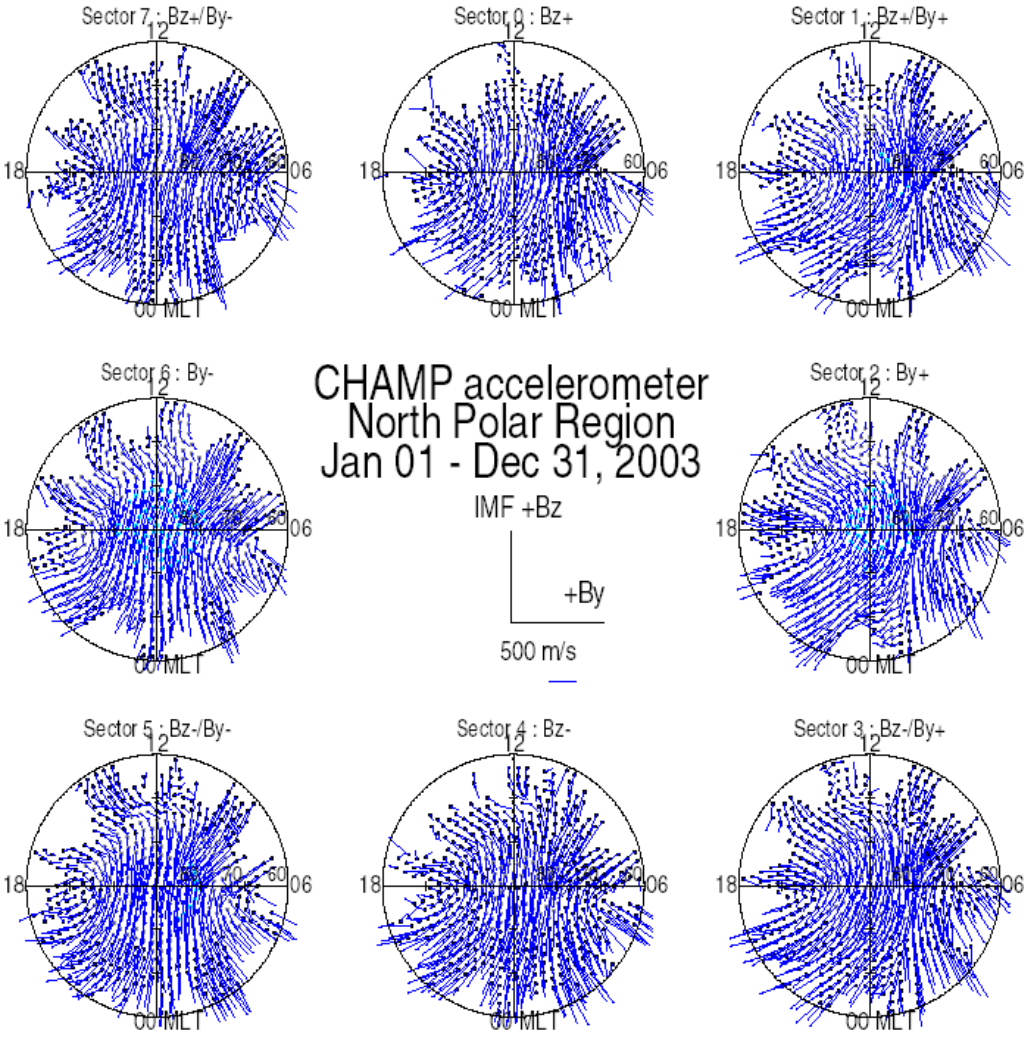

From: Förster et al., *Ann. Geophys.*, **26**, 6, 1581-1595, 2008

Plasma drift (Cluster)

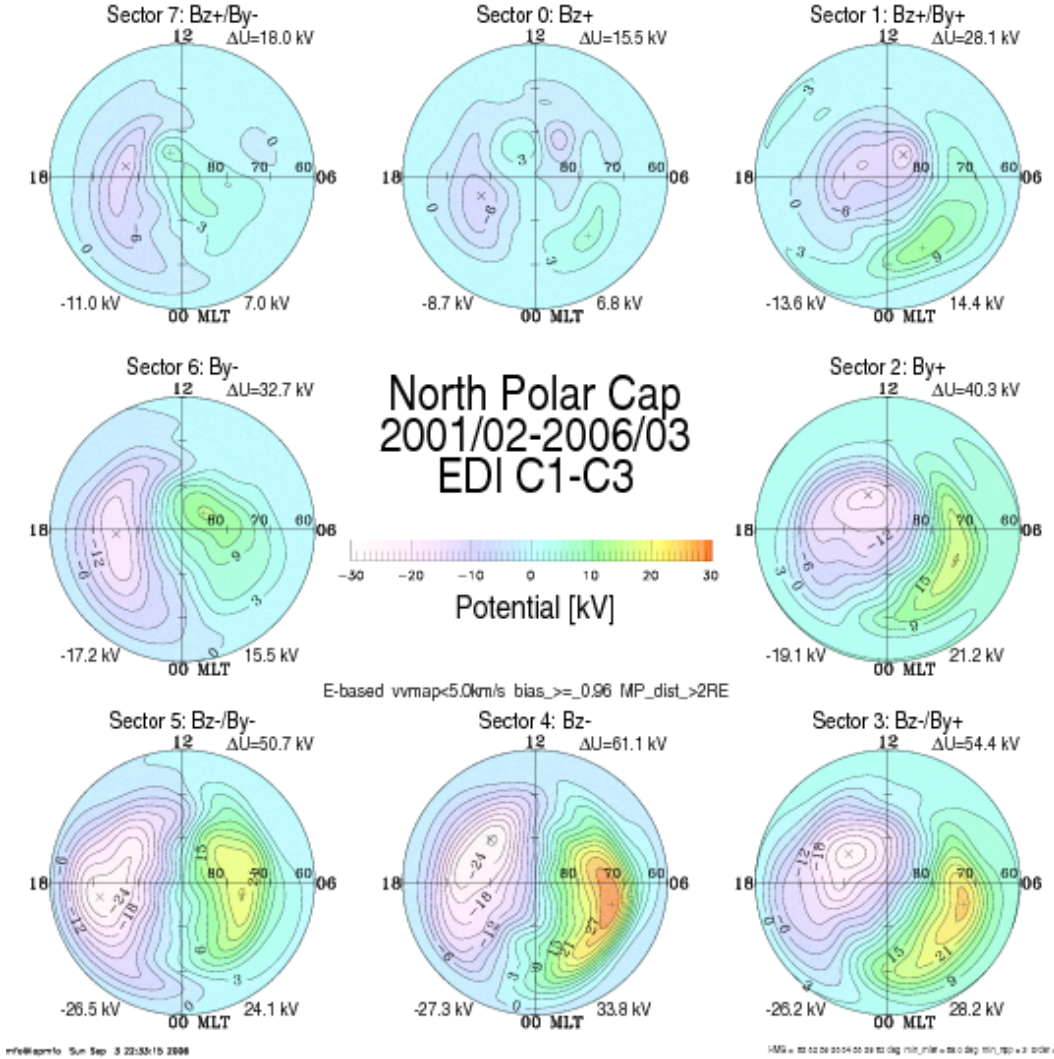

From: Haaland et al., *Ann. Geophys.*, **25**, 1, 239-253, 2007

South Hemisphere

Neutral wind (CHAMP)

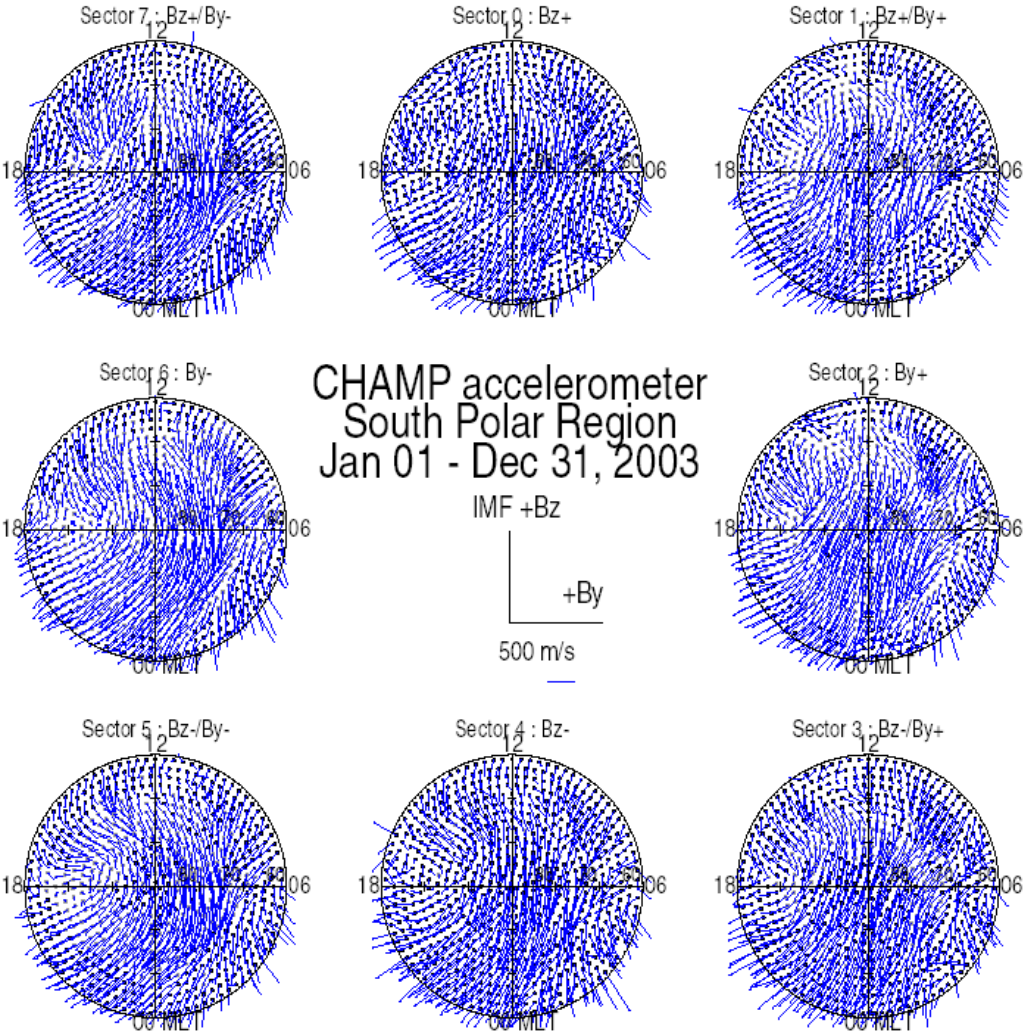

Plasma drift (Cluster)

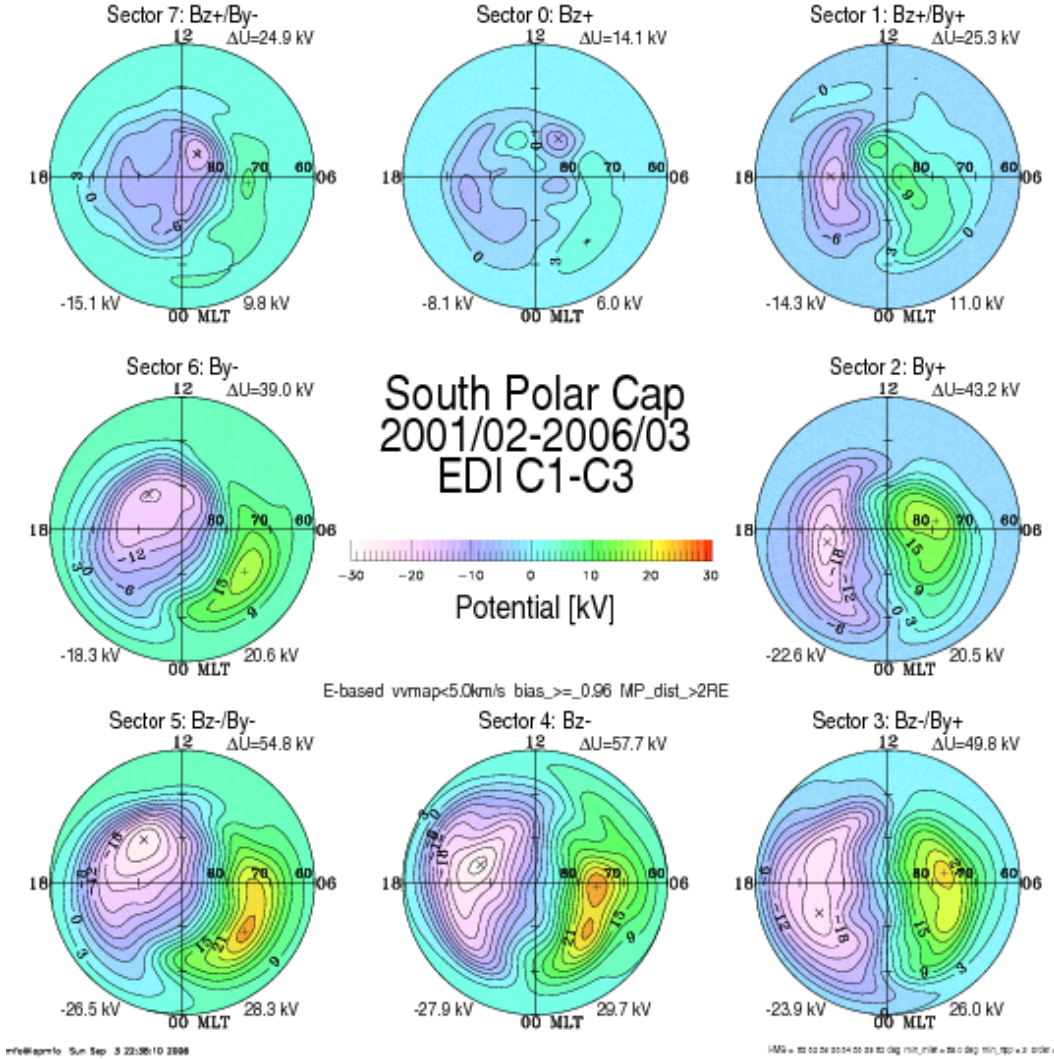

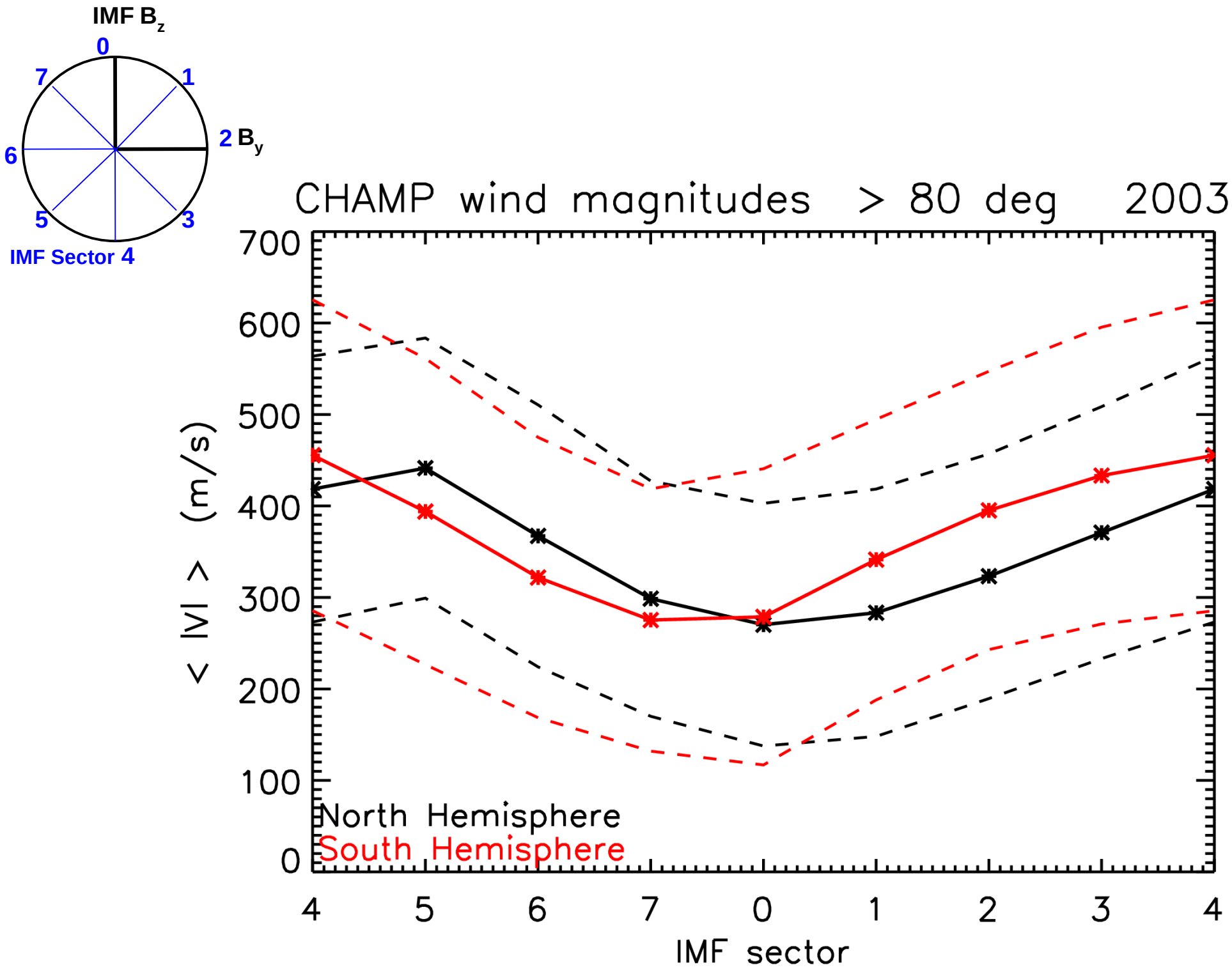
IMF B_z
0
1
2 B_y
3
4
5
6
7
IMF Sector
CHAMP wind magnitudes > 80 deg 2003
< |V| > (m/s)
700
600
500
400
300
200
100
0
North Hemisphere
South Hemisphere
4
5
6
7
0
1
2
3
4
IMF sector

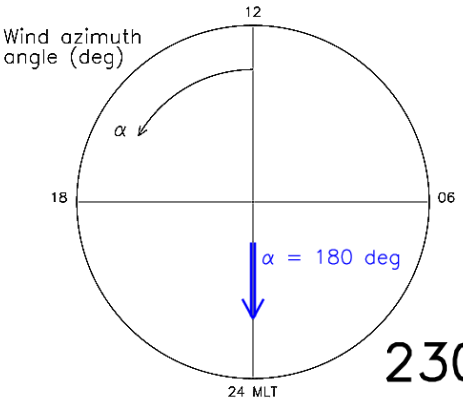

CHAMP wind azimuth > 80 deg 2003

< α > (deg)

230
220
210
200
190
180
170
160

North Hemisphere
South Hemisphere

4 5 6 7 0 1 2 3 4

IMF sector

The Magnetosphere

obstacle in the solar wind

Normal stress:
Chapman-Ferraro currents, dipole interaction

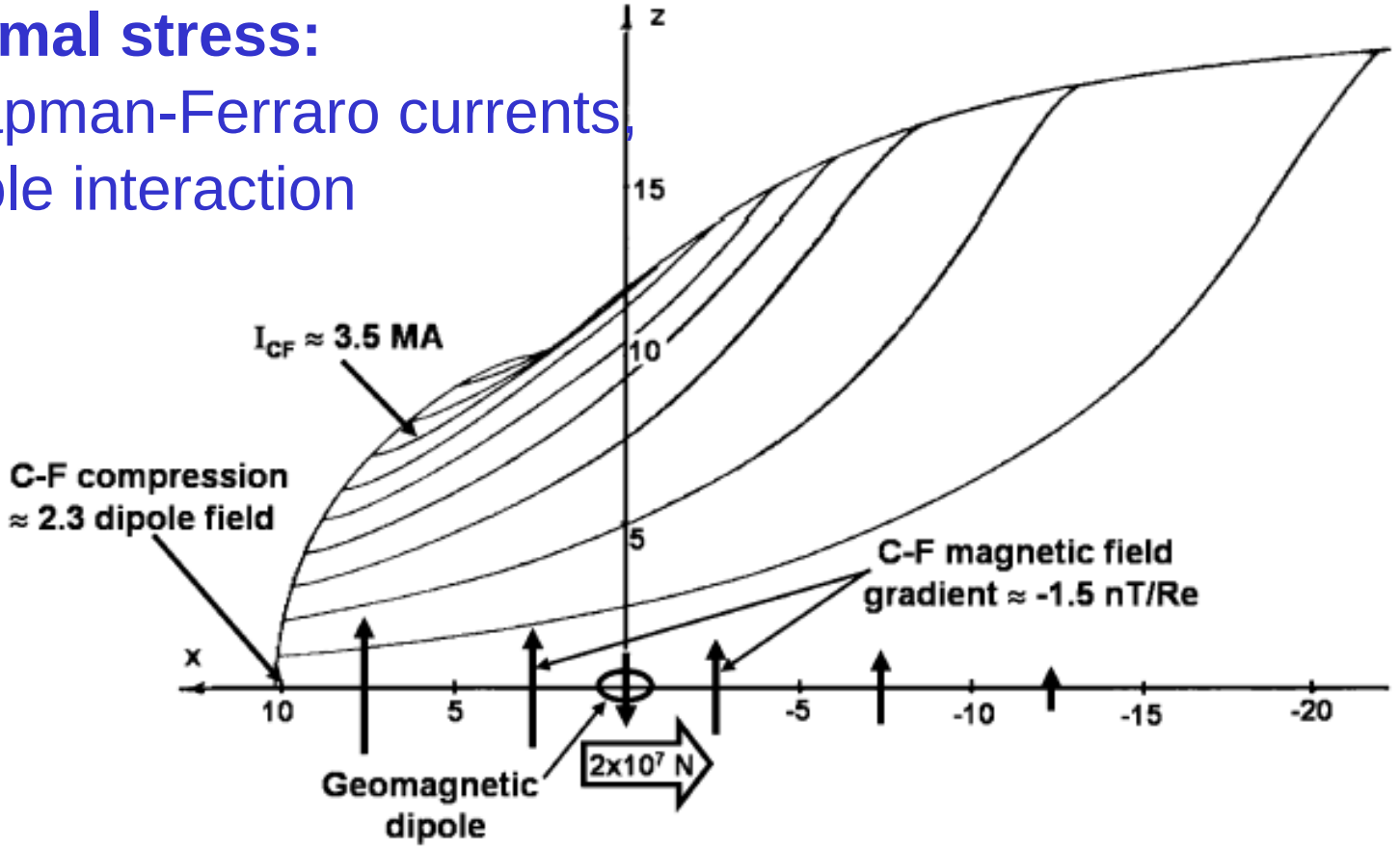

Chapman–Ferraro current lines and associated parameters for IMF = 0 calculated analytically (Midgley and Davis, 1963).

The Magnetosphere

obstacle in the solar wind

Normal (drag force) **&** **Tangential stress** (viscous or Maxwell)

Solar wind with IMF

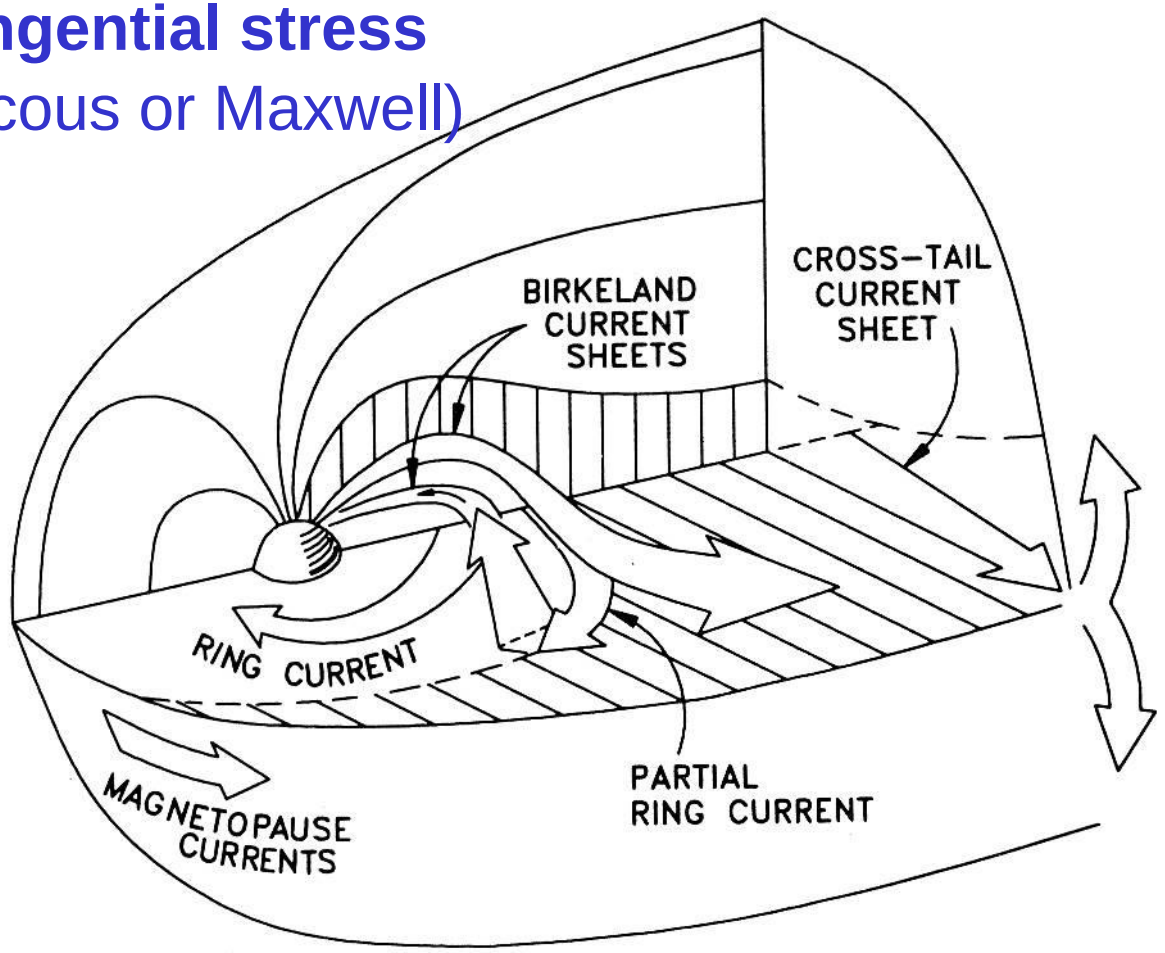

Drivers : Ion Drag & **J** x **B** Force

Region-1 currents are generated at the magnetopause and are closed over the polar cap…

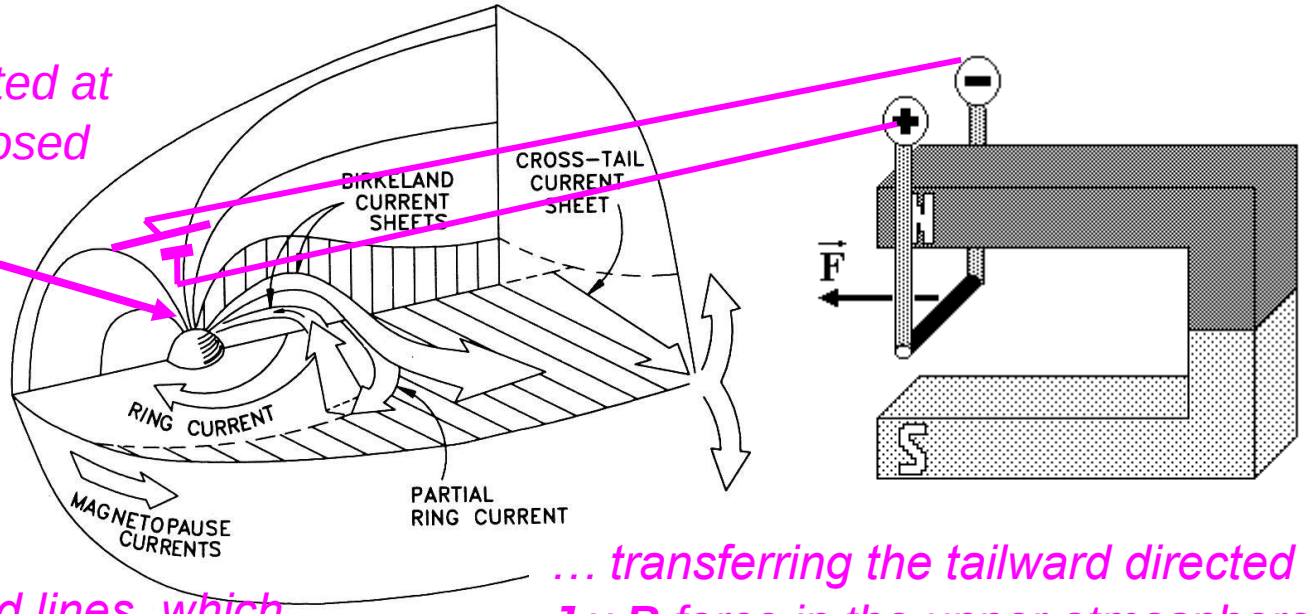

Reconnection at the magnetopause drives large-scale magnetospheric plasma drift …

… via the geomagnetic field lines, which map the plasma drift pattern in the upper ionosphere …

… where magnetic tension from above is balanced against thermospheric drag in the upper atmosphere.

*… transferring the tailward directed **J** x **B** force in the upper atmosphere.*

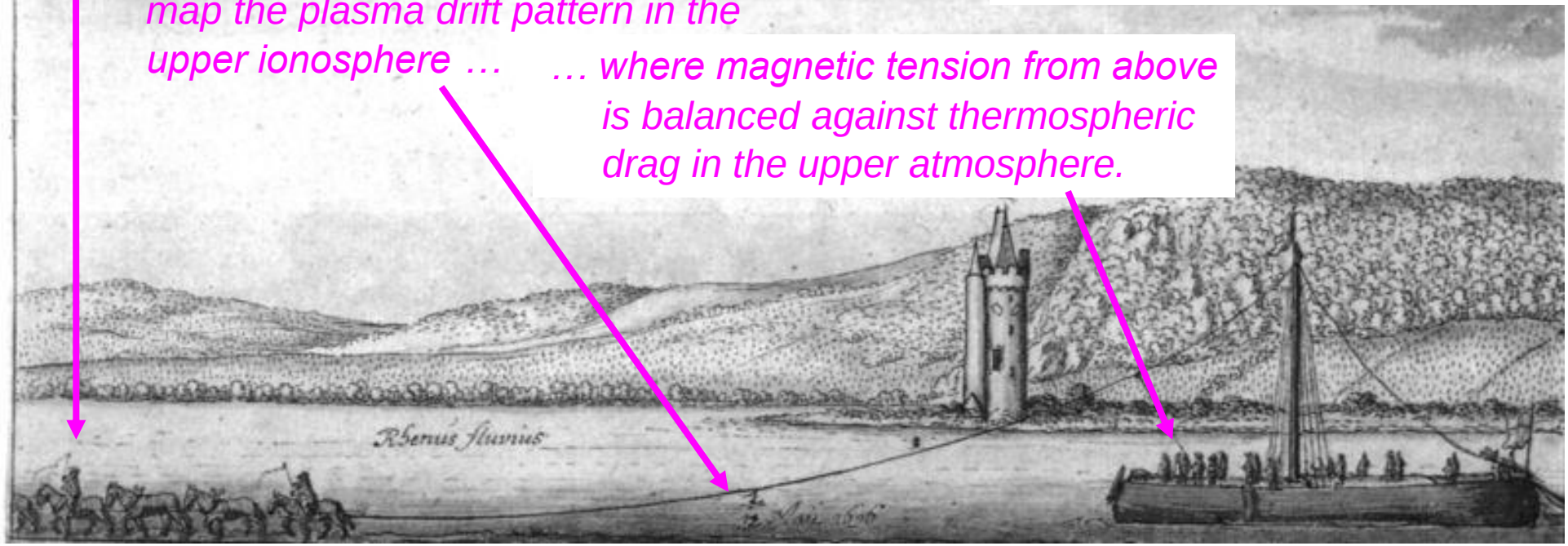

cf. : G.L. Siscoe & K.D. Siebert, *J.Atmos.Terr.Physics*, **68**, 911-920, 2006

Swarm Constellation Mission

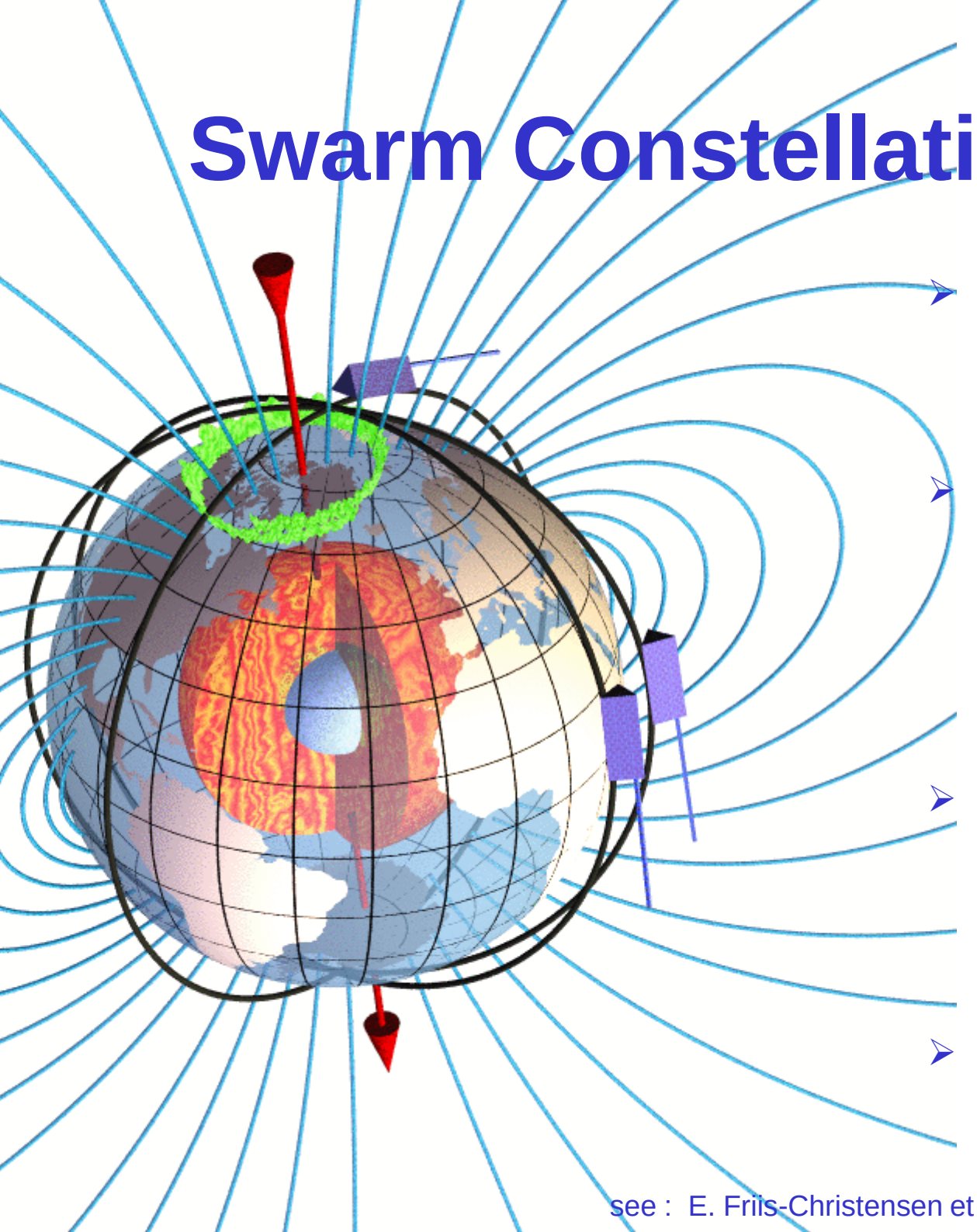

- 5th ESA Earth Explorer Mission: Geomagnetic Research from Space
- Both Earth Interior (core, mantle, and crust) as well as External Sources (magneto-spheric and ionospheric currents)
- Magnetic signatures of the Ocean tides, litospheric mag-netization, e.g., subduction zones, magnetic anomalies…
- Satellite drag for upper atmosphere diagnostics

see : E. Friis-Christensen et al., *EOS Transactions*, **90**, No. 25, 213-214, 2009

Conclusions

- Large-scale clockwise circulation vortices at the dusk side are dominant features for IMF B_y+ conditions at the Northern, and B_y- at the Southern Hemisphere.
- The dawn cell is not favoured for thermospheric wind response of plasma circulation due to counteracting Coriolis- and centrifugal forces.
- Largest magnitudes of cross-polar upper thermospheric winds occur for IMF B_z-/B_y- (sector 5) at the Northern, and B_z-/B_y+ (sector 3) at Southern Hemisphere.
- Larger standard deviations of the wind amplitudes at the Southern Hemisphere in comparison with the Northern ("stirring effect").
- The "pressure valve" effect for the neutral wind is manifested also in smaller angular variations of wind vector directions under these asymmetric conditions.

References:

Haaland, S.E., G. Paschmann, M. Förster, J.M. Quinn, R.B. Torbert, C.E. McIlwain, H. Vaith, P.A. Puhl-Quinn, and C.A. Kletzing, (2007) High-latitude plasma convection from Cluster EDI measurements: method and IMF-dependence, *Annales Geophysicae*, **25**, 239-253.

Förster, M.; Paschmann, G.; Haaland, S. E.; Quinn, J. M.; Torbert, R. B.; Vaith, H.; Kletzing, C. A. (2007) High-latitude plasma convection from Cluster EDI: variances and solar wind correlations, *Annales Geophysicae*, **25**, 7, 1691-1707.

Förster, M.; S. Rentz, W. Köhler, H. Liu, and S. E. Haaland, (2008) IMF dependence of high-latitude thermospheric wind pattern derived from CHAMP cross-track measurements, *Annales Geophysicae*, **26**, 6, 1581-1595.

Doornbos, E., J.Van den Ijssel, H. Lühr, M. Förster, and G. Koppenwallner (2010) Neutral density and crosswind determination from arbitrarily oriented multi-axis accelerometers on satellites, *AAIA*, in press.